# Hand Synergies During Reach-to-Grasp

C. R. MASON, J. E. GOMEZ, AND T. J. EBNER
*Department of Neuroscience and Graduate Program in Neuroscience, University of Minnesota, Minneapolis, Minnesota 55455*

Received 6 February 2001; accepted in final form 17 August 2001

**Mason, C. R., J. E. Gomez, and T. J. Ebner.** Hand synergies during reach-to-grasp. *J Neurophysiol* 86: 2896–2910, 2001. An emerging viewpoint is that the CNS uses synergies to simplify the control of the hand. Previous work has shown that static hand postures for mimed grasps can be described by a few principal components in which the higher order components explained only a small fraction of the variance yet provided meaningful information. Extending that earlier work, this study addressed whether the entire act of grasp can be described by a small number of postural synergies and whether these synergies are similar for different grasps. Five right-handed adults performed five types of reach-to-grasps including power grasp, power grasp with a lift, precision grasp, and mimed power grasp and mimed precision grasp of 16 different objects. The object shapes were cones, cylinders, and spindles, systematically varied in size to produce a large range of finger joint angle combinations. Three-dimensional reconstructions of 21 positions on the hand and wrist throughout the reach-to-grasp were obtained using a four-camera video system. Singular value decomposition on the temporal sequence of the marker positions was used to identify the common patterns ("eigenpostures") across the 16 objects for each task and their weightings as a function of time. The first eigenposture explained an average of 97.3 ± 0.89% (mean ± SD) of the variance of the hand shape, and the second another 1.9 ± 0.85%. The first eigenposture was characterized by an open hand configuration that opens and closes during reach. The second eigenposture contributed to the control of the thumb and long fingers, particularly in the opening of the hand during the reach and the closing in preparation for object grasp. The eigenpostures and their temporal evolutions were similar across subjects and grasps. The higher order eigenpostures, although explaining only small amounts of the variance, contributed to the movements of the fingers and thumb. These findings suggest that much of reach-to-grasp is effected using a base posture with refinements in finger and thumb positions added in time to yield unique hand shapes.

## INTRODUCTION

The hand is a highly complex structure with 27 bones, 18 joints, and 39 intrinsic and extrinsic muscles (Kapandji 1970; Tubiana 1981) with over 20 degrees of freedom (Soechting and Flanders 1997). Movement of the fingers requires a coordinated interplay of both extrinsic and intrinsic muscles (Landsmeer 1963; Landsmeer and Long 1965; Long et al. 1970). This biomechanical complexity raises the question, how does the CNS control the hand and fingers? There are two divergent viewpoints. The more traditional view has emphasized a strategy based on controlling individual muscles and joints to generate the needed forces (for review see Lemon 1999; Schieber 1990). Another view has emphasized the need for "simplifying" strategies that reduce the number of degrees of freedom and thereby reduce the complexity of the control problem (Arbib et al. 1985; Iberall and Fagg 1996; Santello et al. 1998). Recent psychophysical, anatomical, and physiological studies have found support for the latter view.

Considerable evidence supports the concept that the fingers act synergistically with other fingers, with the wrist, and with the arm. Our fingers do not move in isolation of the neighboring fingers (Engel et al. 1997; Flanders and Soechting 1992; Soechting and Flanders 1997) even when the explicit goal is to make individuated finger movements (Schieber 1991, 1995; Schieber and Poliakov 1998). A striking finding in typing and piano playing is that almost all the fingers and joints are in motion simultaneously (Engel et al. 1997; Gordon et al. 1994; Soechting and Flanders 1997). Nor does the hand move in isolation of the arm. Movements of the arm and shaping of the hand during reach-to-grasp are highly coordinated (Bootsma et al. 1994; Chieffi and Gentilucci 1993; Jeannerod 1984; Marteniuk et al. 1990; Paulignan et al. 1990, 1991). Therefore the coordination of the fingers, wrist, and arm indicate that a global control strategy may be utilized.

The anatomy of the finger muscles may simplify the control problem in the primate hand. The low individuation and stationarity of the long fingers shown by Schieber (1991) could be due to the multi-finger insertions of the communal flexor and extensor muscles or reflect part of the CNS's strategy to the control the hand (Santello and Soechting 1997, 1998; Santello et al. 1998). In monkeys, mechanical coupling between fingers by interconnection between tendons and by motor units that exert tension on more than one tendon prevents movement at a single finger level (Schieber 1995; Schieber et al. 1997; Serlin and Schieber 1993). The communal flexor and extensor muscles also cross multiple joints (Kapandji 1970; Tubiana 1981). Therefore biomechanically the control of the individual joints or fingers is limited.

Stimulation studies of the primary motor cortex (MI) have often been cited as supporting evidence that this structure is organized to control individual muscles. Cortical stimulation in humans, apes, and monkeys has yielded the textbook homunculus (Penfield and Rasmussen 1950) or simiusculus (Leyton and Sherrington 1917; Woolsey 1958). However, as reviewed by Schieber (1990) and Lemon (1999), a strict somatotopic organization is not consistent either with earlier or more recent

Address for reprint requests: T. J. Ebner, Dept. of Neuroscience, University of Minnesota, Lions Research Building, Rm. 421, 2001 Sixth St. SE, Minneapolis, MN 55455 (E-mail: ebner001@umn.edu).

The costs of publication of this article were defrayed in part by the payment of page charges. The article must therefore be hereby marked "*advertisement*" in accordance with 18 U.S.C. Section 1734 solely to indicate this fact.

  

stimulation studies. The earliest studies of the hand area within MI found that the cortical territories from which the surface stimulation evokes movement of different digits overlap extensively and that stimulation of one site elicits movement of multiple digits (Leyton and Sherrington 1917; Penfield and Rasmussen 1950; Woolsey 1958; Woolsey et al. 1979). Recent investigations using more refined stimulation techniques have confirmed that contraction of a particular hand muscle can be evoked from a substantial fraction of MI (Andersen et al. 1975; Sato and Tanji 1989). A similar overlapping organization has been found for finger movement (Gould et al. 1986; Kwan et al. 1978; Strick and Preston 1978). Spike-triggered averaging demonstrates that many corticomotoneuronal cells facilitate the electromyographic (EMG) activity of more than one muscle (Buys et al. 1986; Cheney and Fetz 1985; Cheney et al. 1985; Lemon et al. 1986; McKiernan et al. 1998).

Recent inactivation and lesion studies also support the concept that M1 is not organized to perform isolated finger movements (Poliakov and Schieber 1999). Focal muscimol inactivations in the hand region of M1 in the monkey do not disrupt the movements of isolated fingers but instead disrupt movements of different finger combinations (Schieber and Poliakov 1998). Small infarcts in the hand area of human M1 result in weakness of the fingers, but the deficits are not limited to a single digit (Schieber 1999). Therefore M1 does not appear organized around a finely delineated somatotopic map specifying the activation of individual muscles or joints.

Last, recent studies have shown that static grasp posture can be described using a small number of postural synergies (Santello and Soechting 1998; Santello et al. 1998). These synergies could be defined as a spatial configuration or "primitive" of the hand shape that is common across the various tasks. In the latter study, subjects were asked to reach out and grasp imaginary objects. Even without visual or tactile inputs, the hand shapes were distinct (Santello et al. 1998). Using a principal component analysis, the first three components were needed to describe approximately 90% of the variance, with the first two components explaining approximately 84%. Although the individual contributions were small, the higher order components were responsible for more subtle adjustments of the grasp posture (Santello et al. 1998). The evolving hand shape during the transport phase of reach-to-grasp carries increasing information that peaks at the actual object grasp when the hand can conform to the object (Santello and Soechting 1998). The presence of postural synergies that contributed to the evolving hand shaping was not examined, yet the results suggest that a common strategy may control hand shape throughout reach-to-grasp.

Therefore the hand is controlled as a unit at some level and to some degree. The present study asks three questions about these hand synergies. The original description that hand posture can be described by a small number of synergies was based on static hand posture (Santello et al. 1998), yet it is well-known that hand shape evolves throughout reach-to-grasp (Jeannerod 1984; Paulignan et al. 1990). Hence, the first question was whether the entire behavior can be described by a similar small set of synergies and whether these synergies were similar for different types of grasps. These synergies imply a spatial configuration that is not static but is modulated in time to allow subjects to grasp objects of different shapes and sizes. Second, the study of Santello et al. (1998) used mimed grasps of imagined objects. Neither the tactile or visual information was available to the subjects. This prompts the question of whether tactile input or visual input would dramatically alter the hand synergies? Last, based on an information theory analysis, the higher order postural synergies were shown to be important (Santello et al. 1998), but the nature of the contribution was not evaluated. Therefore this study examines how the higher order synergies contributed to the shaping of the hand during reach-to-grasp.

In the present study, subjects performed grasps of 16 objects consisting of 3 classes of shapes including cylinders, cones, and spindles. Within each class the sizes of the object were systematically varied. Five variations of power and precision grasps were studied including actual and mimed grasps. The evolution of the grasp was evaluated in a continuous manner from the initial start position through maintained object contact for each of the different grasps using singular value decomposition (SVD). The results show that the subjects used a base hand shape that explained a large percentage of the variance in hand kinematics throughout reach-to-grasp. This base hand shape was independent of the type of grasp or tactile input. However, additional components were necessary to adequately describe the evolution of the grasp. An abstract describing some of these results has been presented (Mason et al. 1999).

## METHODS

### *Experimental paradigm and procedures*

Five adults (3 women and 2 men, age ranging from 21 to 44 yr old) with no known history of neurological or musculoskeletal problems, participated in the study. All were right-handed as determined by the Edinburgh Handedness Inventory (Oldfield 1971) and had normal hand function. The protocol was approved by the Institutional Review Board of the University of Minnesota, and all subjects gave informed consent.

Each subject performed five different tasks with each object: *1*) Power Grasp, *2*) Power Grasp with a Lift, *3*) Mimed Power Grasp, *4*) Precision Grasp, and *5*) Mimed Precision Grasp. In Power Grasp the subjects were instructed to reach for and grasp the object as if they were going to lift the object using their whole hand making palmar contact. Subjects were to maintain the grip without moving the object until the end of the trial. Power Grasp with a Lift was the same as Power Grasp with the inclusion of the lifting the object approximately 2 cm off the table surface. In the Mimed Power Grasp, the object was moved an additional 40 cm out of the subject's reach. The subjects were to reach as if grasping the object at the standard object location and pantomime a Power Grasp of the object. In Precision Grasp the subjects were instructed to reach for and grasp the object between their thumb pad and four long finger pads as if they were going to lift the object. In the Mimed Precision Grasp, the object was moved 40 cm further away and subjects were to reach as if grasping the object at the standard target location and pantomime a Precision Grasp of the object. During the mimed tasks the subjects had to rely on vision and memory to shape the hand appropriately for each object.

Subjects were seated at a table with their right arm by their side and the elbow flexed to 90° so that the hand rested in a comfortable posture on an "X" located near the edge of the table. For tasks in which the object was actually grasped, the object was placed 30 cm away from the table's edge in the subject's midsagittal plane. For the mimed grasps the object was placed 70 cm away from the table's edge. At 70 cm the object was beyond the subjects' comfortable reaching distance yet was within their visual field.

Before each trial, the subject was instructed orally in the desired grasp for the upcoming trial. The subject indicated the beginning of a

trial by pushing the trigger button of the data collection system with the left hand. The subject reached out with the right hand and performed the requested grasp, maintaining it until hearing a tone indicating the end of 3 s of data collection. The subject then returned his or her hand to the start position. The trials were self-paced. Each subject completed 5 repetitions of the 5 experimental tasks for each of the 16 randomly presented objects. Object presentation was of a block design with the tasks presented randomly for each object. The subject was able to view his or her hand and the object at all times.

Sixteen different wood objects, 12 cm in height, were used (Fig. 1). Object shapes included five cones, five cylinders, and six spindles. The cones had a base diameter of 10 cm and base angles of 67.4, 71.6, 76.0, 80.5, and 85.2°. The cylinders were 5, 6, 8, 9, and 10 cm diam. Each spindle had end diameters of 8 cm with central diameters of 4, 6, 7, 9, 10, or 12 cm. The mean weight of the objects was 187 ± 107 g (mean ± SD; range, 31–385 g).

Prior to the initiation of the data collection, reflective markers 4 mm diam sown to 1-cm$^2$ pieces of nylon fabric were attached with rubber cement to the subject's right hand to record the kinematics of the reach and grasp. Twenty-one positions on the hand and wrist were monitored with markers placed on the second through fifth metacarpophalangeal (MCP) joints, the proximal and distal interphalangeal (IP) joints, and the tips of the fingernail (Fig. 2). In addition, rods with two reflective spheres were taped firmly to the skin, extending vertically away from the hand at the following locations: 8 cm proximal to the wrist crease, wrist crease, thumb MCP, thumb IP joint, and the tip of the thumb. The distance from the center of the top sphere to the desired hand location was measured and entered into the tracking program to create virtual markers on the hand. The rods made it possible to maintain all markers in at least 2 of the 4 cameras throughout the reach and grasp. All markers and rods remained adhered to the skin throughout the data recording.

The kinematics of the reach and grasp were recorded using a video-based motion analysis system (Motion Analysis, Santa Rosa, CA). Prior to each data collection session a two-step calibration procedure was completed. The first step utilized a 12-in. cube with 12 precisely located markers placed in the middle of the workspace. A 60-s data file was collected. The second step utilized a wand with three reflective markers, the outer two separated by 200 mm. The wand was moved throughout the workspace so that it was viewed both in the horizontal and vertical planes by all four cameras for 120 s. The tracking software utilized the two calibration techniques to establish the location of each camera and account for any geometric distortion introduced by the camera lenses. Marker positions were sampled at 60 Hz using four video cameras. Using the tracking software the marker positions were tracked for the 3-s duration of the reach-to-grasp. Each trial was checked for correct identification of markers and edited as required. The tracked data were then filtered using a Butterworth filter

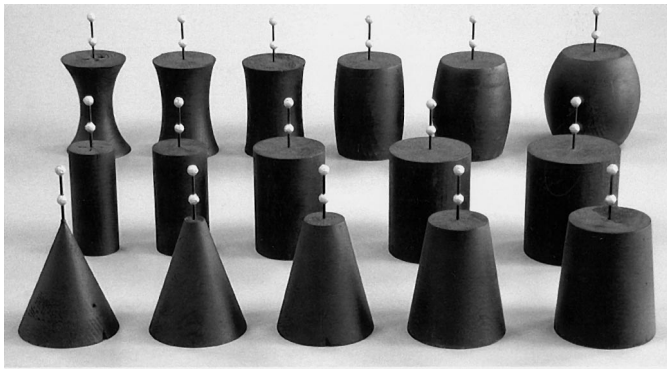

FIG. 1. The 16 objects are shown grouped by shape and increasing in size from the *left* to the *right*. The wooden objects were painted flat black to reduce the glare. The rods with reflective markers extending from each object were used to provide their location in the work field.

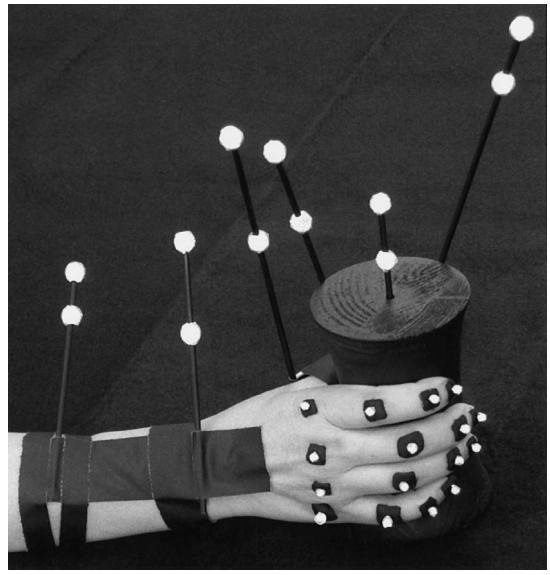

FIG. 2. A view of *subject 4*'s hand with the reflective markers and rods during a power grasp of a spindle. Note that the rods make it possible to monitor the thumb position even though the thumb is not in this camera view. Each marker needed to be visible to a minimum of 2 cameras for successful 3-dimensional (3-D) reconstruction of its location in space throughout the reach and grasp.

with the cutoff set at 6 Hz, and exported to SAS (SAS Institute, Cary, NC) for further processing. The velocities of the *x*, *y*, and *z* positions of the wrist crease virtual marker were determined by numerical differentiation. Tangential velocity was the vector summation of the resultant *x*, *y*, and *z* velocities.

Each reach was normalized using movement onset and offset as the break points. Movement onset was defined as the time when the tangential velocity of the wrist crease marker exceeded 1 cm/s. Analogously, movement offset was defined as the time when the tangential velocity of the wrist crease marker dropped below 1 cm/s. The marker position data were then interpolated to fill 60 bins for each epoch, the initial hold position, the reach, and the object grasp for a total of 180 bins. The wrist crease marker was defined as the origin (0, 0, 0), and all markers were redefined in relation to the wrist marker. Orientation of the wrist and hand in space was maintained by the preservation of the three-dimensional (3-D) position of the markers relative to each other. The five grasps of each task for each object were then averaged. The averaged grasps for each subject were analyzed by task using SVD.

### *Analyses*

Singular value decomposition analysis was used to analyze the evolving hand postures throughout the reach-to-grasp (Hendler and Shrager 1994). Similar to principal component analysis (Glaser and Ruchkin 1976), SVD reduces the data into a linear combination of orthogonal hand postures, referred to as "eigenpostures" in which the variance explained by each successive eigenposture diminishes progressively. One advantage of SVD is that it also provides information on the temporal evolution of the hand postures, therefore permitting a determination across time. Calculation of the SVD was based on the matrix X (2,880 × 63) constructed of the *x*, *y*, and *z* positions of the 21 hand markers beginning with the 1st bin on the initial hold and continuing until the final bin of the object grasp for a total of 180 bins for each of the 16 objects. Matrix X was then deconvolved into three matrixes, $X = U\Sigma V^T$. Matrix U (63 × 63) consisted of the patterns of the marker positions that defined the eigenvectors (i.e., eigenpostures). Matrix V (2,880 × 2,880) consisted of the temporal weightings of the eigenpostures, a sequence of values that defined the contribu-

tion of each eigenposture throughout the reach-to-grasp. The superscript T denoted the transpose. Last, $\Sigma$ (2,880 $\times$ 63) was a diagonal matrix consisting of the eigenvalues for the eigenposture-temporal weighting pair in a greatest-to-least order. The eigenvalues indicate the relative amount of variance explained by each eigenposture-temporal weighting pair. The variance is obtained by squaring the eigenvalues and dividing by the sum of squares. The SVD analysis was completed for each task separately to be able to explicitly compare the eigenpostures generated for the different tasks. The comparison was essential to determine whether the same hand synergies were generated during the various tasks (e.g., power vs. precision).

Eigenpostures and hand shapes were visualized using 3-D rendering software [Persistence of Vision Ray Tracer (POVray)] to render 3-D images. The images were created by entering the *x*, *y*, and *z* values for each position as a sphere and linking the appropriate spheres with cylinders to form the hand shapes. Within POVray, it is possible to change the camera's perspective and lighting of the 3-D object. However, the same camera perspective and lighting was maintained for all of the first eigenpostures and hand reconstructions. The camera was rotated 180° around the *x*-axis for improved clarity of the second eigenposture.

Two methods of comparison of the eigenpostures of the different tasks and their respective temporal weightings were undertaken. The root mean square (RMS) difference for the 21 marker positions between the E1s of the various tasks was calculated to quantify the similarities between the eigenpostures. The RMS differences were calculated for each subject and averaged. A statistical comparison of the eigenpostures was based on two sample Student's *t*-tests of the means of the marker positions of the eigenpostures between tasks. The temporal weightings provide information about the hand shaping through time. In addition to plotting the weightings as a function of time, phase plane plots of the temporal weightings from the first two eigenpostures were created. Plots of the phase plane trajectories for the five tasks for different objects were used to address the question of whether the different grasps fall within the same or different regions of the phase plane space.

As shown in RESULTS, the amount of variance explained by successive eigenpostures decreases sharply after the first eigenposture (E1), with higher eigenpostures explaining only small incremental amounts of variance. To determine the nature of the information provided by the higher order eigenpostures, a series of reduced versions of the original data matrix were constructed using the inverse of the SVD formula. Reduced versions of the original data matrix were calculated using only the 1st eigenposture, eigenvalue, and temporal weighting, the 1st and 2nd eigenpostures, eigenvalues and temporal weightings, and so on, up to including the 1st 10 eigenpostures, eigenvalues, and temporal weightings. The reduced version of the matrix was compared with the actual hand posture both visually and by computing the RMS error as a function of time.

## RESULTS

### *SVD analyses across grasps for all subjects and objects*

The SVD analyses show that the vast majority of the variability in the hand posture for the entire act of reach-to-grasp can be described by a small number of eigenpostures. The first eigenposture (E1) accounts for 97.3 $\pm$ 0.89% (mean $\pm$ SD) of the variance of the grasp across tasks and subjects, and E2 accounts for 1.9 $\pm$ 0.85% (Table 1). The first three eigenpostures of any grasp describe over 99.5% of the variance. Extending the earlier findings on static hand posture (Santello et al. 1998), these results demonstrate that hand shape throughout reach-to-grasp can be described by one dominant eigenposture and a small number of additional ones.

The first eigenpostures (E1) of the power grasp for the five subjects are shown in Fig. 3. The E1s are remarkably similar for the different subjects. E1 consists of an open grasp configuration in which all the joints are slightly flexed, midposition in the joint range of motion. Qualitatively E1 appears to be the position of function as defined by Kapandji (1970). From this position the hand can either close for smaller objects or open for larger objects. There are slight differences that are due in part to hand size. In Fig. 3 the subjects are ordered by hand size with the largest hand on the left and smaller hands to the right. The fingers of the first two subjects are more flexed than the fingers of the other subjects. The fifth subject who has the smallest hand has the most extended fingers. The gradual decrease in finger flexion from the largest hand to the smallest hand reflects the excursion of the fingers necessary for the different subjects to grasp the 16 objects. The smaller hands are near their peak aperture for a greater portion of the objects than are the larger hands. The similarity in the E1s suggests a common strategy of an open hand configuration that allows for easy adjustment for larger or smaller objects.

The temporal weighting profiles of E1 show how the open hand configuration evolves throughout the reach, shaping the hand for the 16 objects (Fig. 3). A common feature across four subjects is that the weighting increases then decreases throughout the reach in preparation for object grasp. These changes in temporal weighting constitute the larger changes in hand shaping that occur during reach. Notice that the change in the weightings begins at the onset of the reach and reflects the previously described shaping of the hand in preparation for the grasping of an object (Jeannerod 1984; Paulignan et al. 1990). The fifth subject tended to rest her hand in a more open position than the other subjects did. This subject also had the smallest hand, so there was little additional extension that occurred in the reach. This difference is reflected in the weightings, which do not show the initial increase. The shape of this profile is object-dependent, demonstrating a unique grasp posture for each object. The temporal weightings continue to change during the beginning of the object grasp period, reflecting adjustments in the grasp as the object is contacted.

During the initial hold period the temporal weightings are relatively constant, indicating that the hand shape was relatively constant. The differences in the weightings of the initial hold period reflect the very early initiation of the hand shaping that precedes the onset of reach as noted previously (Jeannerod and Biguer 1982). The weightings during the object grasp period are also constant but differ as a function of the object, again an indication of a unique hand shape for each object. The variability of the weightings in the three periods suggests that the subjects not only controlled this basic hand shape during the reach-to-grasp but prior to the reach and after object grasp.

The first eigenposture is similar for the five different grasps. As shown in Fig. 4 for *subject 1*, E1 for each type of grasp consists of an open hand configuration with the fingers slightly flexed and the thumb in opposition to the palm. Again, E1 explains the vast majority of the variance (97.2 $\pm$ 1.2%) for the five tasks for *subject 1*. The major differences in E1 are a function of whether the grasp was power or precision, with the power grasp having more open shape with overall flexion of the fingers. Also the thumb is more flexed in the three power grasps than in the precision grasps. This increased flexion of the thumb and long fingers is likely to represent preparation for making palmar contact with the object by wrapping the thumb

TABLE 1. *Amount of variance explained by each eigenposture for each subject by task*

| Subject | Task | E1 | E2 | E3 | E4 | E5 | E6 | E7 | E8 | E9 | E10 |
|---|---|---|---|---|---|---|---|---|---|---|---|
| *1* | Power | 98.0 | 1.42 | 0.272 | 0.129 | 0.057 | 0.053 | 0.027 | 0.020 | 0.008 | 0.004 |
| | Power with Lift | 97.5 | 1.79 | 0.381 | 0.176 | 0.065 | 0.034 | 0.022 | 0.020 | 0.007 | 0.004 |
| | Mimed Power | 97.2 | 2.18 | 0.248 | 0.152 | 0.124 | 0.035 | 0.025 | 0.014 | 0.009 | 0.004 |
| | Precision | 98.2 | 1.49 | 0.121 | 0.067 | 0.046 | 0.035 | 0.007 | 0.007 | 0.003 | 0.003 |
| | Mimed Precision | 95.2 | 4.44 | 0.164 | 0.080 | 0.037 | 0.017 | 0.012 | 0.006 | 0.004 | 0.002 |
| *2* | Power | 97.1 | 1.78 | 0.762 | 0.220 | 0.047 | 0.031 | 0.018 | 0.012 | 0.011 | 0.005 |
| | Power with Lift | 97.8 | 1.62 | 0.310 | 0.189 | 0.047 | 0.019 | 0.009 | 0.007 | 0.007 | 0.005 |
| | Mimed Power | 96.9 | 1.51 | 1.31 | 0.132 | 0.040 | 0.024 | 0.019 | 0.012 | 0.009 | 0.008 |
| | Precision | 97.8 | 1.61 | 0.302 | 0.199 | 0.049 | 0.022 | 0.009 | 0.007 | 0.007 | 0.006 |
| | Mimed Precision | 98.1 | 1.37 | 0.316 | 0.123 | 0.042 | 0.03 | 0.016 | 0.012 | 0.006 | 0.004 |
| *3* | Power | 96.3 | 2.59 | 0.659 | 0.192 | 0.076 | 0.045 | 0.020 | 0.018 | 0.013 | 0.008 |
| | Power with Lift | 96.4 | 2.53 | 0.626 | 0.200 | 0.093 | 0.033 | 0.018 | 0.014 | 0.009 | 0.008 |
| | Mimed Power | 97.2 | 1.88 | 0.473 | 0.214 | 0.067 | 0.037 | 0.022 | 0.019 | 0.012 | 0.008 |
| | Precision | 96.2 | 3.10 | 0.282 | 0.155 | 0.078 | 0.064 | 0.018 | 0.015 | 0.007 | 0.006 |
| | Mimed Precision | 96.5 | 2.90 | 0.322 | 0.146 | 0.057 | 0.031 | 0.019 | 0.014 | 0.009 | 0.008 |
| *4* | Power | 97.6 | 1.52 | 0.563 | 0.121 | 0.066 | 0.053 | 0.030 | 0.012 | 0.009 | 0.007 |
| | Power with Lift | 97.3 | 1.62 | 0.543 | 0.331 | 0.061 | 0.05 | 0.030 | 0.011 | 0.009 | 0.007 |
| | Mimed Power | 95.6 | 3.45 | 0.663 | 0.150 | 0.061 | 0.043 | 0.028 | 0.014 | 0.010 | 0.008 |
| | Precision | 98.3 | 1.10 | 0.391 | 0.071 | 0.047 | 0.031 | 0.026 | 0.008 | 0.006 | 0.005 |
| | Mimed Precision | 97.2 | 2.12 | 0.421 | 0.093 | 0.057 | 0.035 | 0.022 | 0.006 | 0.004 | 0.004 |
| *5* | Power | 97.3 | 1.48 | 0.975 | 0.117 | 0.054 | 0.038 | 0.023 | 0.014 | 0.008 | 0.007 |
| | Power with Lift | 97.4 | 1.48 | 0.908 | 0.084 | 0.052 | 0.028 | 0.021 | 0.017 | 0.009 | 0.007 |
| | Mimed Power | 98.6 | 0.718 | 0.384 | 0.169 | 0.061 | 0.052 | 0.011 | 0.006 | 0.004 | 0.003 |
| | Precision | 98.2 | 1.28 | 0.278 | 0.131 | 0.051 | 0.023 | 0.013 | 0.008 | 0.006 | 0.005 |
| | Mimed Precision | 98.7 | 0.933 | 0.218 | 0.105 | 0.043 | 0.023 | 0.008 | 0.003 | 0.003 | 0.002 |
| | Mean | 97.3 ± 0.895 | 1.92 ± 0.847 | 0.476 ± 0.282 | 0.15 ± 0.059 | 0.059 ± 0.019 | 0.035 ± 0.012 | 0.019 ± 0.007 | 0.012 ± 0.005 | 0.008 ± 0.003 | 0.006 ± 0.002 |

Values in Mean are means ± SD.

and fingers around the object. Conversely, the more extended finger and thumb flexion for the precision tasks may represent preparation for finger pad opposition during object contact. The similarities of the E1s across tasks and subjects demonstrate that modulation of this one postural synergy can account for much of the hand shaping.

The modulation of this basic hand shape as a function of task time can be appreciated in the E1 temporal weightings (Fig. 4). The overall profile is consistent across objects and grasps with an increase in the weight after reach onset followed by a decrease, reflecting the hand opening and closing in preparation for object grasp. The temporal weightings of the eigenpostures diverge prior to the reach and continue to separate throughout the reach and remain separated at the completion of the reach. The weightings are different for each of the 16 objects, indicating a unique grasp for each of the objects as shown for the power grasp across all subjects (Fig. 3). Again the differences in the weightings during the initial hold period reflect the early preshaping of the hand prior to reach onset.

The largest differences in the temporal weightings are between the mimed grasps and the corresponding actual grasps. Although the increase-decrease profile occurs across the grasps, the change is compressed for the mimed grasps. The subjects did not open or close their hands to a similar extent when contact was not required. The differences in the weightings for the power grasp with and without the lift suggest that the subject used a slightly different hand posture when the tasks required that only contact be made with the object versus when the object had to be lifted. To accomplish the lift, the subject would need to apply opposing forces with fingers, palm, and thumb during the lift to adequately counteract the tangential pull of gravity. The fluctuations of the weights near the time of object grasp may reflect subtle adjustment in the grasp.

The E2 of the power grasp for the five subjects suggests that it contributes to the control of the thumb and long fingers (Fig. 5). These eigenpostures are illustrated with the camera rotated 180° around the *x*-axis from the perspective used in Figs. 3 and

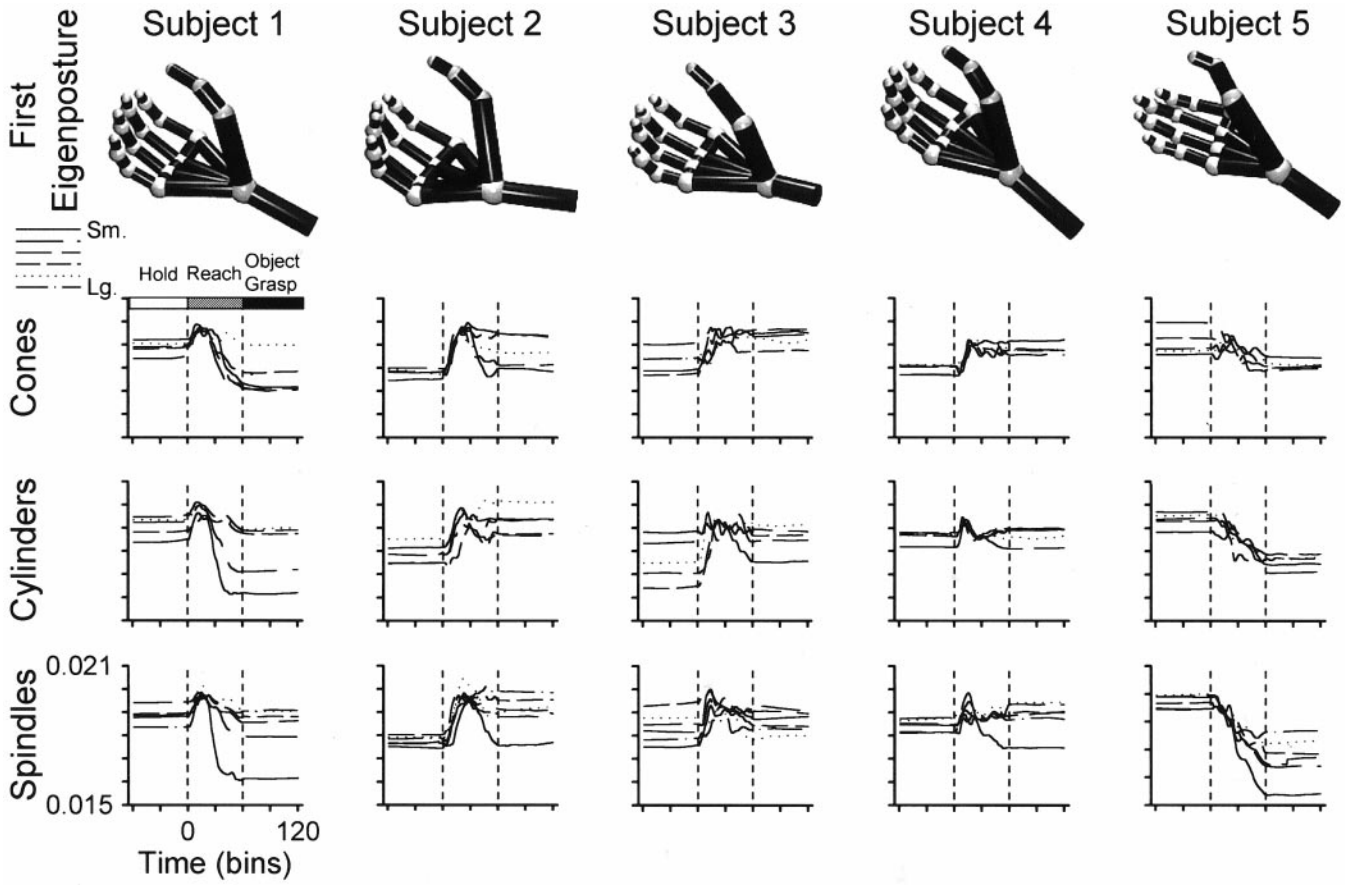


FIG. 3. The E1s and temporal weightings for the 5 subjects for power grasp. The temporal weighting profiles of the eigenpostures for each of the 16 objects are shown below the eigenpostures. For ease of comparison, the temporal weightings are separated by object shapes with cones in the 1st row, and cylinders in the 2nd and spindles in the 3rd row. Above the *top left plot* is the task time line including initial hold, reach, and object grasp periods, and the dotted vertical lines provide a similar division. The *x*-axes are normalized time bins. See text for greater detail.

4 for better viewing of the posture. The proximal and distal phalanges of the thumb are pointing toward the reader (numbered 1 in Fig. 5) with the MCP of the thumb away from the reader. The MCP of the little finger is toward the reader. The fingers cross each other so that the second digit is pointing toward the reader and the fifth digit away from the reader. Likewise, the third and fourth fingers are crossed so that the fingertips are in the inverse order of the MCPs. The same inversion of the fingertips in relation to the MCPs is present in the E2 of *subjects 2*, *3*, and *4*. In *subject 5*'s E2 the crossover occurs from the wrist joint. This difference may be due to the size of this subject's hand in relation to the other subjects.

The thumbs of *subjects 2* and *4* are more prominent than that of *subject 1*, suggesting that their thumb positioning may contribute more to the aperture of the hand than for other subjects. The thumbs of *subjects 3* and *5* are smaller than the thumbs of the other subjects and also shorter relative to the other fingers in their respective eigenpostures; again this may reflect differences in positioning of the thumb by the subjects. E2 explains a small portion (1.9 ± 0.84%) of the variance across subjects and tasks. By definition E2 is orthogonal to E1, and the shape reveals that this is not a natural or physiological hand posture. Subjects cannot easily configure their hands to the postures shown in E2. However, the E2s do provide insight into the independent control that must be applied to the fingers and thumb and added to E1 to produce the complete configuration of hand postures the subjects achieve.

The temporal profiles of the E2 weightings are similar to the profiles of E1 for each subject. At the beginning of reach, the weighting increases reflecting the opening of the hand to its maximum aperture. In *subjects 1*, *3*, and *5* the temporal weightings then decreased as the hand closed in on the object. In *subjects 2* and *4*, the decrease in the temporal weightings after maximum aperture were less pronounced. The temporal weightings plateaued during object grasp at different levels reflecting the hand posture required for the different objects. Therefore even though E2 has more individual variability than E1, there are similarities in the shapes and the temporal weightings.

The E2s across the different tasks are shown for one subject and explain on average of 2.3 ± 1.25% of the variance (Fig. 6). As described for the E2 of the power grasp of *subject 1* previously, the order of the fingertips is inversed in relation to the order of the MCPs for the E2 of the power grasp with a lift, precision grasp, and the two mimed grasps. The thumb is prominent for the power grasp, power grasp with a lift, and the precision grasp and less prominent for the mimed grasps. The E2s for the two mimed grasp tasks are similar to the grasp of actual objects (Fig. 6). The E2 temporal weightings follow the same profile as the E1 weightings (Fig. 4) except for the mimed

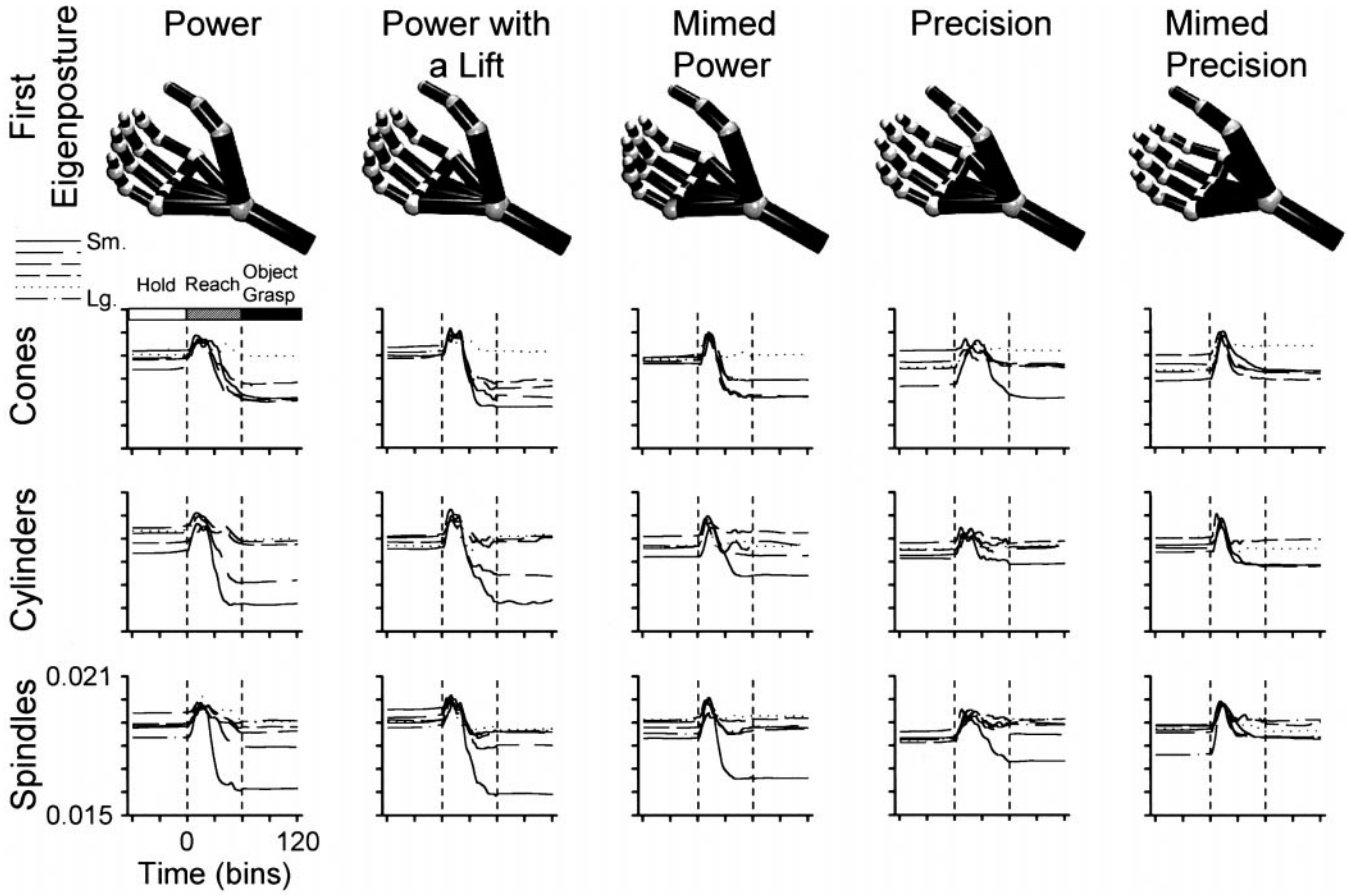


FIG. 4. The E1s and the temporal weightings for the 5 tasks for 1 subject. The E1s for the 5 tasks are illustrated in the *top row*. Notice the similarities in the hand postures across the task. Below each eigenposture the weightings of the eigenpostures are shown for each object. Each object has a unique weighting within each task. The weighting are similar for the power grasp and power grasp with a lift, 2 tasks which are essentially the same but are unique for the other tasks. Conventions as in Fig. 3.

precision grasp. For the other four tasks the weights during the initial hold are constant. The weights increase with onset of the reach then decrease in anticipation of the object grasp. The weights again are constant during the object grasp. For the mimed precision task the weights during the initial hold are constant. In contrast to the other four tasks, the temporal profile of the E2 weighting for the mimed precision grasp has an initial increase during the onset of the reach that plateaus and remains constant during the object grasp. Again the weighting differences indicate that the grasp posture for each of the 16 objects is unique.

Among the five tasks, only the power grasp with a lift required an efficient grasp with force application adequate to overcome gravity during the lift. In the other tasks the subjects were requested to grasp the objects as if they were going to lift them. However, the forces were not monitored, and the subjects could have conformed their hands to the objects without the force application. To quantify the similarities between the E1 of power grasp with and without a lift, the RMS differences were calculated. The RMS differences between the E1s for the two tasks indicate negligible differences considering the difference is across the *x*, *y*, and *z* locations of 21 markers for each eigenposture. For *subject 1* the difference was 0.024 mm (Table 2). The average difference across all subjects was $0.024 \pm 0.019$ (Table 2). Similarly, the differences between the E2s for the two tasks were negligible (Table 2). A two-sample *t*-test of the eigenpostures between the two tasks did not show a significant difference ($P > 0.05$) for either the E1s or the E2s. These small and insignificant differences indicate that the eigenpostures for power grasp with and without a lift are the same irrespective of the forces utilized.

The average RMS differences between all tasks for E1 and E2 are summarized in Table 3. The differences between the E1s of the five tasks are small, ranging between $0.024 \pm 0.02$ mm and $0.11 \pm 0.07$ mm. The differences were greatest between the power and precision grasps, particularly between the actual and mimed grasps. However, none of the differences were significant ($P > 0.05$). Similarly, the RMS differences between E2 for the different tasks are small, and the differences between tasks are not significant ($P > 0.05$). The lack of significant differences between the eigenpostures would imply that the same base posture is used for the five tasks with the higher order eigenposture adding further shaping information.

To determine whether power and precision grasps are discrete postures or fall along a continuum, phase plane plots of the temporal weightings of the first two eigenpostures for the five tasks were constructed. Figure 7 shows representative phase plane plots for the different grasps of the smallest, intermediate, and largest cones (*left column*), cylinders (*middle column*), and spindles (*right column*). The trajectories of the phase plane plots are similar for the different tasks and different sizes of cones, cylinders, and spindles. For the smallest

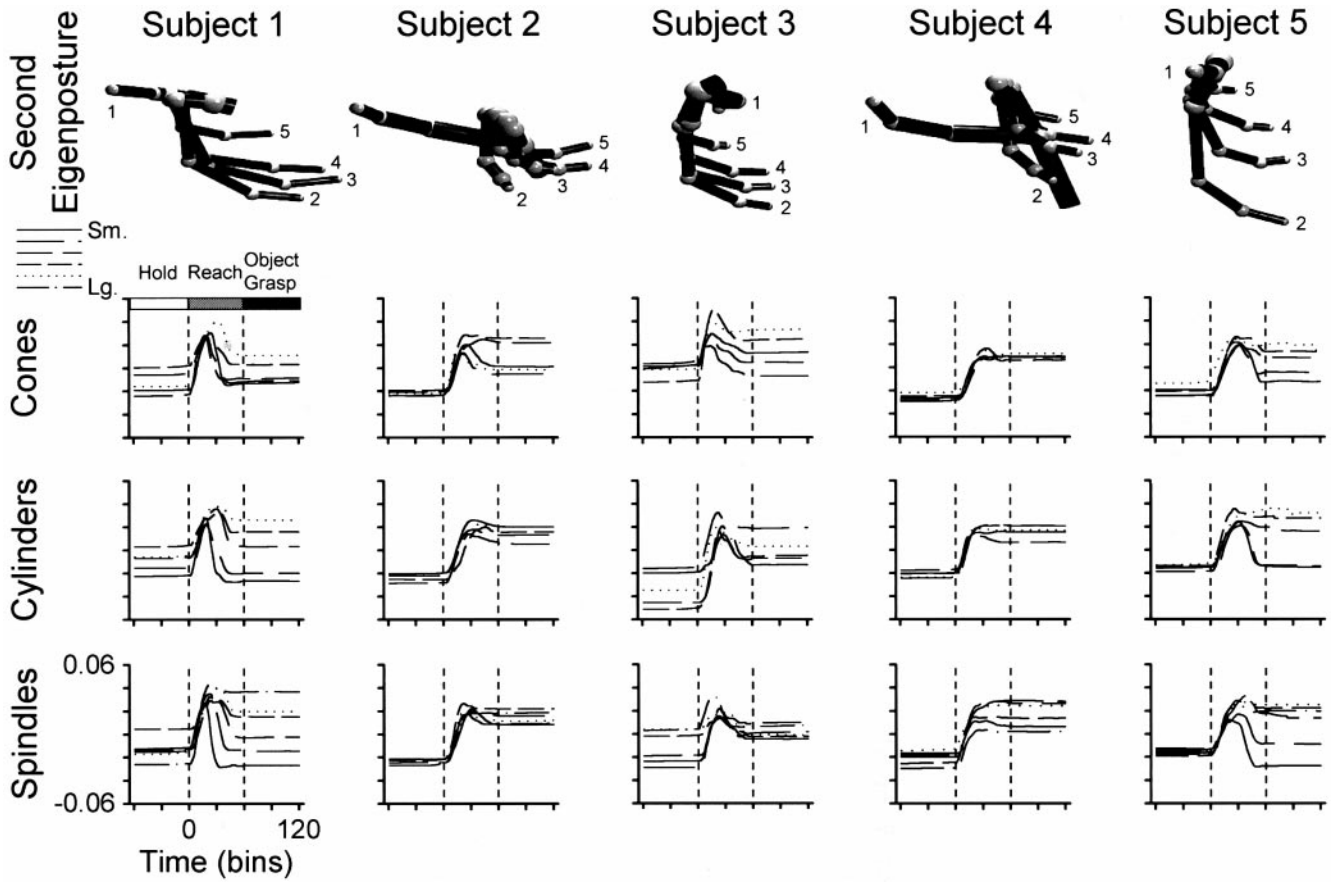


FIG. 5. The E2s and the temporal weightings for the 5 subjects for power grasp. By definition E2 is orthogonal to E1. The camera perspective has been rotated 180° around the *x*-axis. The tips of the fingers are numbered beginning with the thumb as 1 and ending with the little finger as 5. Other conventions as in Fig. 3.

cone the trajectories begin in the bottom left quadrant and move toward the top right quadrant as the hand opens in early reach. The maximum aperture of the hand occurs at the point where the trajectories change direction in the top right quadrant. The trajectories for the three power grasps, power without a lift (thin black line), power with a lift (dark gray line), and mimed power (dotted line), begin to move back toward the bottom left quadrant as the hand encloses the cone. The trajectories of the two precision grasps, precision (thick black line) and mimed precision (light gray line), do not move as far to the left as the hand does not close to the same degree during precision grasp. For the intermediate and large cone the trajectories of the power grasps do not move as far toward the left bottom quadrant after attaining maximum aperture, indicating that the fingers flex less to enclose the intermediate and large cones than they did for the smallest cone. All the trajectories for the largest cone are similar, indicating that the hand posture for the power grasps and precisions grasps approaches the same aperture for *subject 2*. All the trajectories indicate by the small movements at the end of the trajectories that final adjustments in hand shape occur as the object is grasped.

The phase plane plots of the temporal weightings of the first two eigenpostures of *subject 4* for the five tasks in the *middle column* and of *subject 1* in the *right column* are also similar for the five tasks for each size cylinder (*middle column*) or spindle (*right column*). The trajectories start near the bottom of the graph, move upward to the right for the hand opening, and move to the left as the hand closes on the objects. More flexion is indicated during the grasp of the smallest objects by the movement of the trajectories movement further toward the left than for the intermediate and large objects. The hand closure in the power and the precision grasp must be comparable for the cylinders as the trajectories end in the same region of the phase plane. The clustering and similarities of the temporal weighting profiles for the five tasks for each object indicates that power and precision grasps fall along a continuum rather than in discrete regions of the phase space.

### *Contribution of higher order eigenpostures*

Eigenpostures of order >2 contribute only a small fraction of the variability in the hand posture (Table 1). E3 through E10 combined contribute 0.09 ± 0.18% of the variance. On the basis of information theory, it was shown that these higher order components are significant (Santello et al. 1998) but the nature of the contribution remained undefined. Therefore we evaluated how hand shape changed as the higher order eigenpostures were successively added and calculated the RMS differences between the reconstructed shape and the actual hand shape. In Fig. 8 is shown the reconstructed hand shape for *subject 1* performing the power grasp of the smallest spindle. A comparison of the hand postures in the *top* and *bottom rows* at two points in time, bin 15 at the time of peak hand velocity and bin 60 at the beginning of object grasp, illustrates the contri-

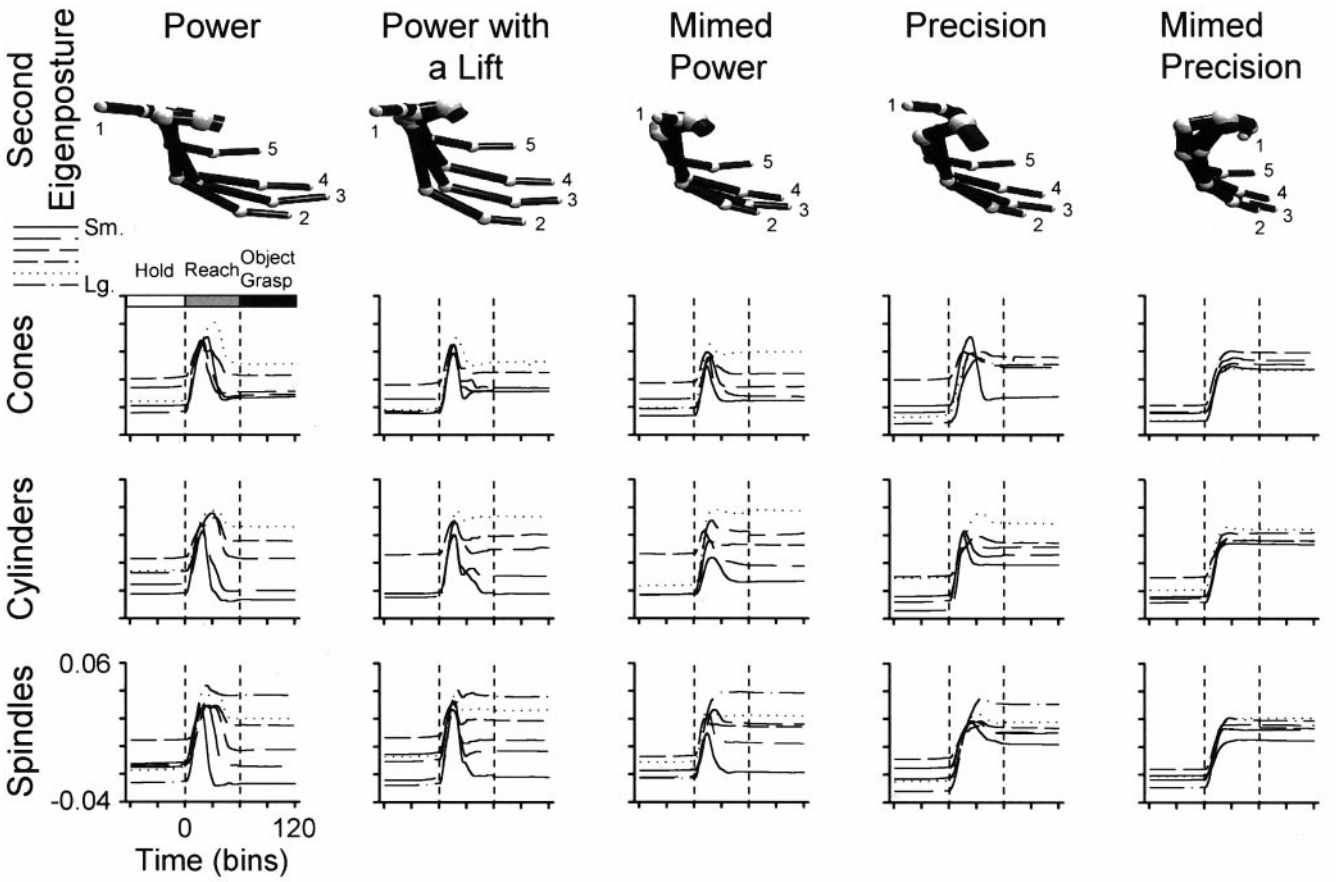


FIG. 6. The E2s and the temporal weightings for the 5 tasks for 1 subject. Finger numbering as in Fig. 5. Other conventions as in Fig. 3. This is the same subject shown in Fig. 4.

bution of the higher order eigenpostures. At peak velocity the hand posture based on only E1 lacks the finger and thumb extension of the true hand posture illustrated in the *bottom row*. Note the large increase in thumb and finger extension with the addition of E2, consistent with the shape of E2 (Figs. 5 and 6). Adding successive eigenpostures further refines the posture of the thumb and fingers. Much of the finger extension occurs at the proximal interphalangeal joints (PIPs) and distal interphalangeal joints (DIPs) accompanied by some extension of the MCPs. This increase in extension occurs in parallel across the three rows of joints (MCPs, PIPs, and DIPs for fingers and MCP and IP joint of the thumb) and not at a single joint level. Therefore the additional eigenpostures provide the finer details of thumb and finger extension that occurs at the maximum aperture of the true hand posture.

At the onset of object grasp (bin 60), the hand shape based only on E1 is lacking the finger and thumb flexion used to grasp the objects. With the addition of E2 the finger and thumb are almost in opposition due to the increased flexion of the thumb and fingers, again showing that E2 is involved in the control of the thumb and fingers. Adding successively E3 to E7 to the reconstruction progressively increases the flexion of the MCPs, PIPs, and DIPs. Again, the increasing flexion occurs in parallel across all joints. After the addition of all the eigenpostures up to and including E7, the flexion of the long fingers closely approximates the flexion observed in the true hand posture. Therefore qualitatively E2–E7 provide information about the state of the flexion/extension of the MCPs, PIPs, and DIPs, even though these eigenpostures explain only a small fraction of the variance.

TABLE 2. *RMS differences between eigenpostures of power with and without a lift*

| | *Subject 1* | *Subject 2* | *Subject 3* | *Subject 4* | *Subject 5* | Mean |
|---|---|---|---|---|---|---|
| E1 | 0.024 | 0.005 | 0.021 | 0.057 | 0.014 | 0.024 ± 0.02 |
| E2 | 0.208 | 0.064 | 0.113 | 0.357 | 0.301 | 0.208 ± 0.123 |

Values in Mean are means ± SD. RMS, root mean square.

To quantify the importance of the higher order eigenpostures, the reduction in the RMS error with the addition of successive eigenpostures was determined. This reduction in RMS error is shown graphically in Fig. 9 for the five different grasps of the smallest spindle by *subject 1*. The RMS error for reconstruction based on E1 is constant during the initial hold. The error decreases briefly as the hand begins to open and the finger extension of the actual hand and the $USV_1$ reconstruction more closely approximate each other. The error increases markedly around peak velocity when the fingers and thumb lack adequate extension for the maximum aperture. The error decreases after the maximum aperture as the fingers begin to flex in preparation for the object grasp. Again the true finger posture and the $USV_1$ reconstructed hand shape are relatively close then the RMS error increases as the reach continues and throughout the grasp period because the actual fingers flex in preparation for the grasp and during the grasp but the fingers of the $USV_1$ reconstruction do not.

TABLE 3. *Summary of RMS differences across subjects*

| | Power | Power with Lift | Mimed Power | Precision | Mimed Precision |
|---|---|---|---|---|---|
| | | | *E1* | | |
| Power | 0 | | | | |
| Power with Lift | 0.024 ± 0.020 | 0 | | | |
| Mimed Power | 0.066 ± 0.020 | 0.082 ± 0.033 | 0 | | |
| Precision | 0.070 ± 0.028 | 0.080 ± 0.021 | 0.079 ± 0.020 | 0 | |
| Mimed Precision | 0.099 ± 0.075 | 0.111 ± 0.070 | 0.078 ± 0.054 | 0.069 ± 0.049 | 0 |
| | | | *E2* | | |
| Power | 0 | | | | |
| Power with Lift | 0.209 ± 0.123 | 0 | | | |
| Mimed Power | 0.329 ± 0.226 | 0.442 ± 0.316 | 0 | | |
| Precision | 0.241 ± 0.084 | 0.328 ± 0.057 | 0.367 ± 0.252 | 0 | |
| Mimed Precision | 0.389 ± 0.198 | 0.471 ± 0.284 | 0.249 ± 0.095 | 0.317 ± 0.199 | 0 |

Values are means ± SD. RMS, root mean square.

The addition of successive eigenpostures reduces the error in all phases of the reach-to-grasp. This error reduction is not by an equivalent amount in all phases, indicating that each eigenposture is contributing to different aspects of the hand shape. The inclusion of E2 adding the needed finger and thumb extension results in a particularly larger reduction in the error during the reach for the five grasps. E2 also contributes substantially to the error reduction in the initial hold period (particularly in the mimed grasps) and in the object grasp period for the power grasps. E2 contribution is primarily in the needed flexion of the fingers and thumb during object grasp. The addition of successive higher order eigenpostures results in a decrease of the RMS error. The reduction in error plateaus after the addition of E7 for the power grasp. The RMS errors for the other grasps show a similar reduction in the RMS error with the addition of successive higher order eigenpostures. The error

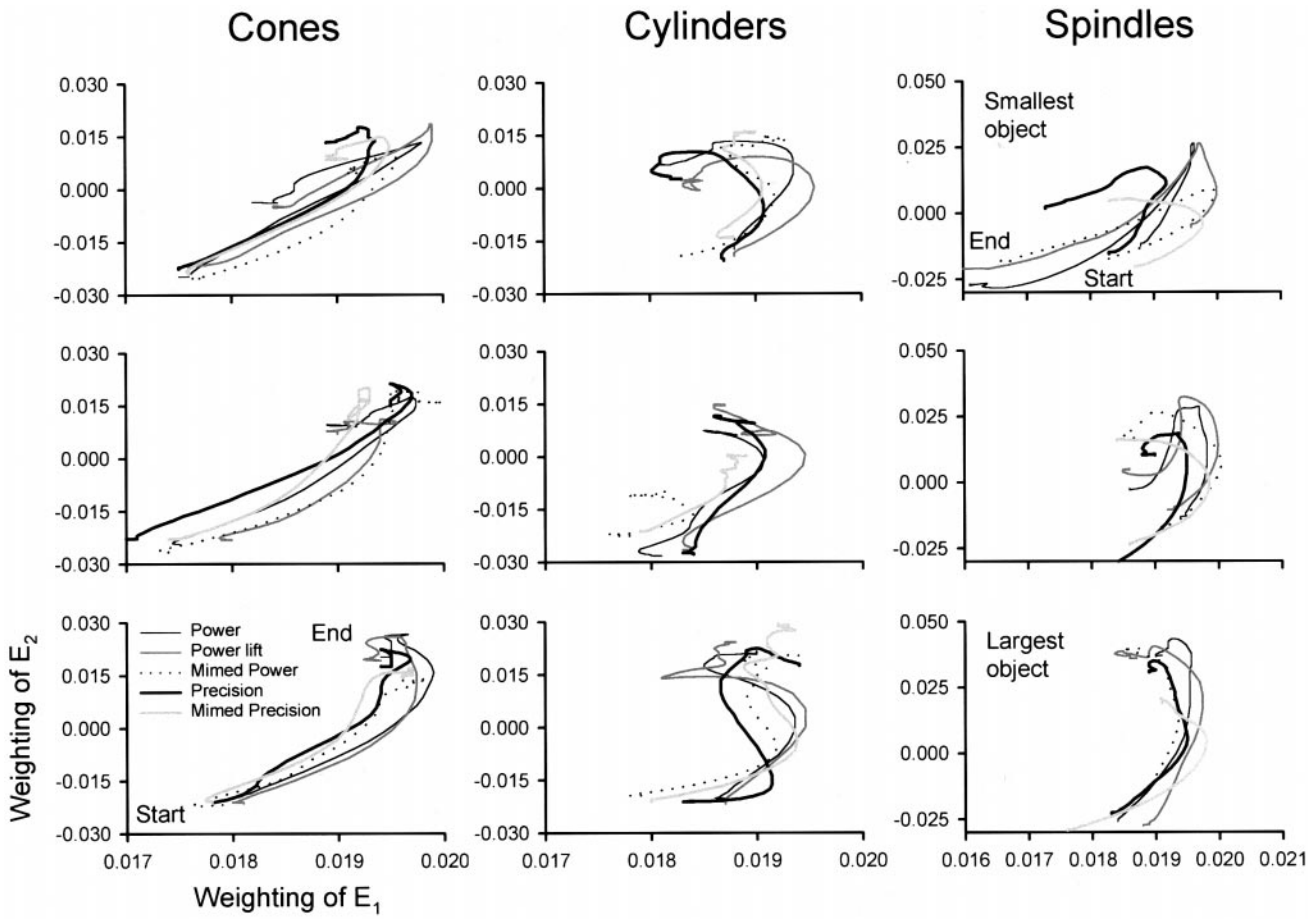


FIG. 7. Phase plane plots of temporal weighting of E1 against the temporal weighting of E2 for the 5 tasks for the smallest (*top*), intermediate (*middle*), and largest (*bottom*) object in each shape. The data in each column are from a different subject. The cones are based on data from *subject 2*, the cylinders from *subject 4* and the spindles from *subject 1*.

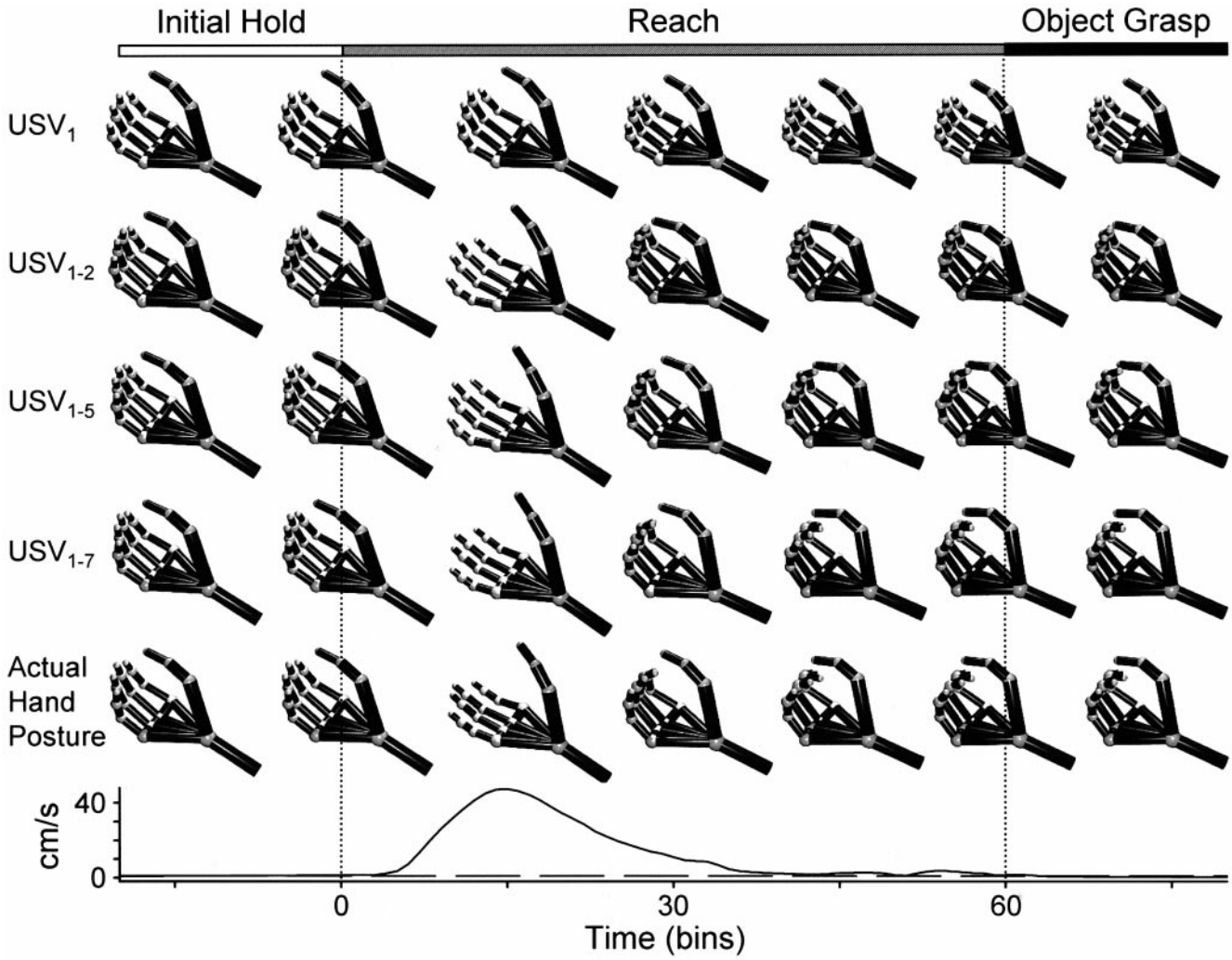


FIG. 8. Hand reconstructions. The *1st 4 rows* depict the hand postures reconstructed from increasing numbers of eigenpostures in the power grasp of the smallest spindle by *subject 1*. The *bottom row of hands* depicts the actual hand postures. Both the reconstructed and actual hand postures are shown at 15 bin intervals. The graph illustrates the normalized tangential velocity of the reach to grasp movement. The solid line depicts the tangential velocity of the wrist. The dashed line represents 1 cm/s. Reach onset occurs when the tangential velocity exceeds 1 cm/s, and reach offset occurs when tangential velocity drops below 1 cm/s.

reduction generally plateaus after the addition of E7 or E8, indicating that the higher order eigenpostures do provide important information even though they only explain a small portion of the variance.

When the RMS error is averaged for the 16 objects across the 5 subjects, the progressive reduction of error with each additional eigenposture is evident (Fig. 10). Again, the error reduction occurs in the three task periods. The fluctuation in the error reduction during the reach is indicative of the evolving hand shape, and the different hand shaping components the higher order eigenpostures add to the evolving hand shape. The error reduction plateaus after the addition of the seventh or eighth eigenposture.

As was stated in METHODS, the SVD analysis was completed for each task separately to be able to compare explicitly the eigenpostures generated for the different tasks. When the SVD analysis was performed across the 5 tasks and 16 objects, the results were similar to those of the SVD analysis by task. The E1 accounts for an average of 97 ± 0.52% of the variance and E2 accounts for 1.93 ± 0.63%. Furthermore, the hand shape based on this analysis across tasks was similar to the SVD analysis on the individual tasks. The RMS difference between the E1 across all tasks and objects and the E1 for each task averages 1.99 ± 0.002 across all subjects. For E2 the RMS difference is 1.94 ± 0.04. Therefore including all grasps does not result in far more significant eigenpostures nor changes the shape defined by the eigenpostures.

## DISCUSSION

In this study the subjects performed 5 different grasp tasks to grasp 16 objects. The SVD analysis of the hand shapes for each grasp indicates that E1 explains most of the variance in the hand shape. The E1s were comparable across subjects and the five tasks, demonstrating that to grasp with precision or power, with or without lift, in the actual or the mimed condition, a common base posture is used. The reconstruction demonstrated that E2 contributes to the opening of the hand to the maximum aperture during reach and thumb and finger flexion during closure of the hand in preparation for object grasp. E2 was

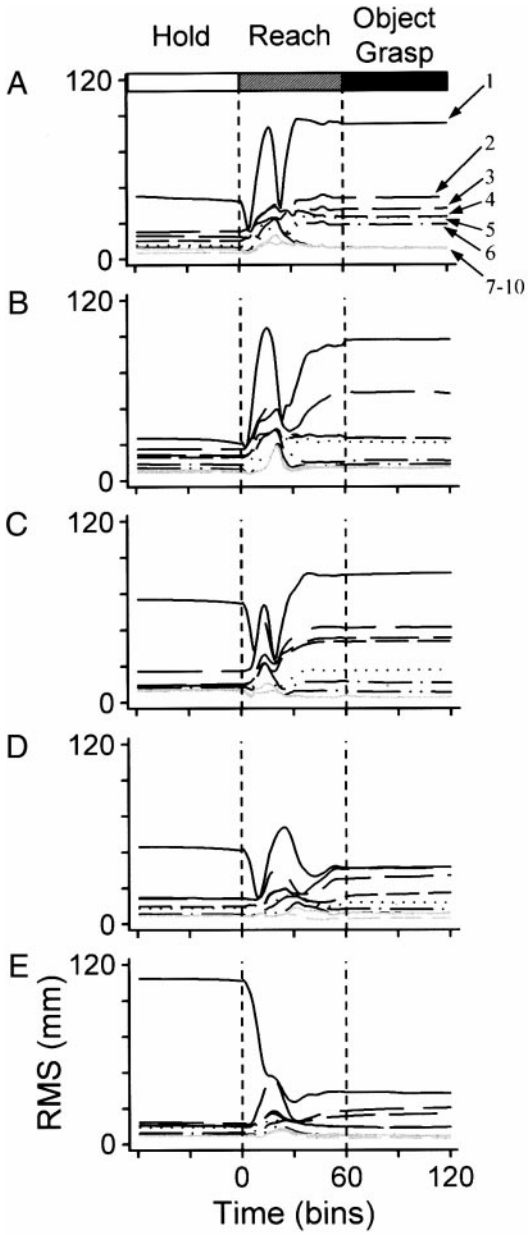


FIG. 9. The root mean square (RMS) error for the 5 grasps of the smallest spindle for *subject 1*. The *top graph* corresponds to the hand reconstructions observed in the preceding figure. The solid line indicates the RMS error using only E1 in the reconstruction. The numbered arrows indicate the highest eigenposture included in the reconstructed matrix on which the RMS error is calculated. Note the consistent drop in error as the higher order eigenpostures are sequentially added in the 5 tasks. *A*: Power Grasp. *B*: Power Grasp with a Lift. *C*: Mimed Power Grasp. *D*: Precisions Grasp. *E*: Mimed Precision Grasp.

more variable across subjects and suggests that there may be independent control over some aspects of grasp, particularly thumb and finger extension. The higher order eigenpostures add further shaping information to the hand shape. These results are comparable to earlier findings that over 80% of the variance of static grasp postures can be explained by two principal components with the higher order components providing additional information (Santello et al. 1998).

The grasp tasks in this study were initially classified as either power or precision as defined by Napier (1956). Napier concluded that prehensile movements consisted of two discrete patterns of movement that identified the grip as either a power grip, a precision grip, or a combination of the two. The grip was determined by how the object was to be used (Napier 1956). Numerous subsequent studies have proposed even more elaborate categorical schemes (Cutkowsky and Howe 1990; Kamakura et al. 1980). The similarities of the eigenpostures for the five different grasps in a subject suggest that only one movement pattern exists even though the final hand posture is dependent on function (or desired grasp) and object to be grasped. The similarities in the phase plane trajectories of E1 and E2 temporal weightings further show that the "classic" Napier precision and power grips were not evident in the grasps and objects explored. Rather than two or more discrete grasps, hand posture may be composed of a continuum based on the temporal weighting of a few eigenpostures. In this case, eigenpostures would not be limited to or be expected to cor-

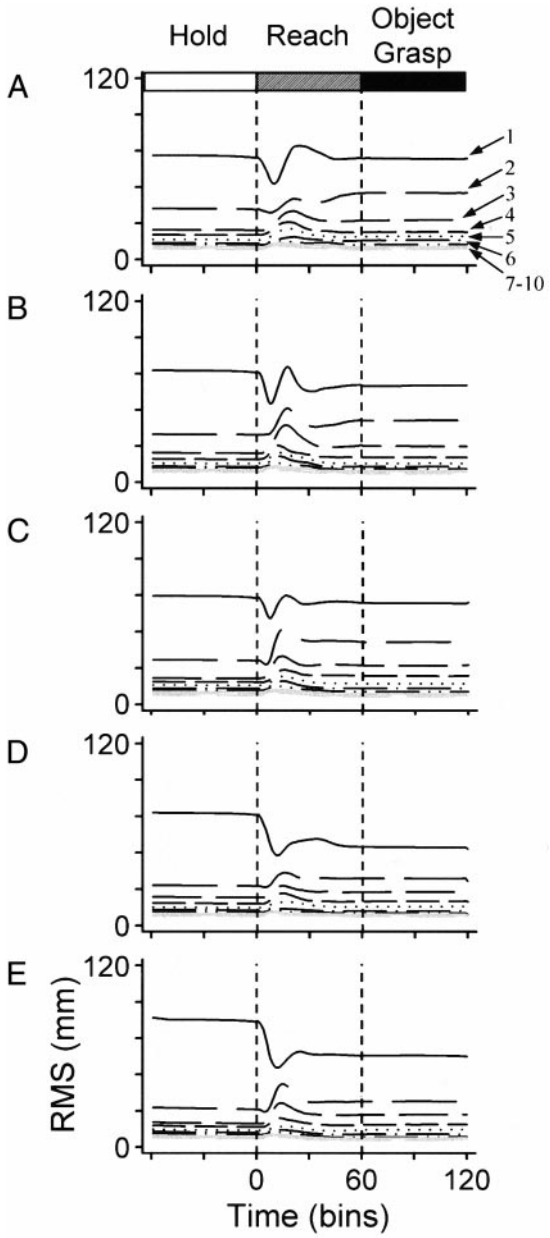


FIG. 10. The average RMS error for the 5 subjects and 16 objects for each of the grasps. Conventions as in Fig. 9.

respond to particular grasps. Two caveats must be considered. First, that power and precision grasps are within discrete regions of the same manifold and the SVD analysis failed to distinguish between the two types of hand shapes. Second the results are limited to the set of objects grasped and the grasps studied. There remains the possibility that if a larger range of grasp behaviors was evaluated a more readily apparent division would develop.

The temporal weightings of the eigenpostures demonstrated that hand shape evolves continuously throughout the reach-to-grasp and is unique for each object/grasp combination. The SVD analysis is a technique to quantify the modulation of the hand shape that begins prior to the reach-to-grasp and continues through to the object contact in the actual grasps or the end of movement in the mimed grasp. The temporal weightings more precisely define the shaping of the fingers for grasp than just the linear scaling of the maximum hand aperture to the object size as previously noted (Chieffi and Gentilucci 1993; Jeannerod 1984; Marteniuk et al. 1990; Paulignan et al. 1990). These results confirm and expand on the finding that hand shape evolved gradually throughout the movement (Santello and Soechting 1998).

A normal open hand posture configuration characterizes E1 and is qualitatively similar to the position of function (Kapandji 1970). However, as noted in RESULTS, E2 is not a natural hand posture but an orthogonal posture to E1. With the large number of degrees of freedom in the hand and with the equally significant biomechanical constraints, it is difficult to conceive of two orthogonal postures that the hand could readily assume. The same problem exists for other dimensionality reduction approaches, and the early study did not show the second or higher principal components (Santello et al. 1998). However, E2 and the higher components do provide insight into the additional finger and thumb movements that are required to shape the hand. The eigenpostures may represent a simplifying scheme used by the CNS to control the hand.

### *Evolution of synergies throughout reach-to-grasp*

The shaping of the hand evolves throughout the reach, beginning with extension of the fingers and thumb followed by flexion in anticipation of object contact (Jeannerod 1984; Paulignan et al. 1990; Santello and Soechting 1998). The temporal weightings show that evolution of the synergies was consistent irrespective of object shape, grasp, or subject. In general there was a biphasic pattern to the weightings, first increasing during the reach then decreasing as the hand closes in on the object. At maximum hand aperture with thumb and fingers extended, the thumb and fingers begin to flex in preparation for object grasp. This general pattern of opening and closing is further evidence that the hand acts as a functional unit. There also appears to be coordinating actions across the MCPs, the PIPs, and the DIPs, in which the fingers extend or flex together. Others have also observed a high degree of correlation in joint angles (Santello and Soechting 1998; Santello et al. 1998). This is further evidence that the hand functions as a unit.

Our results indicate that the hand posture, if not constrained, differs for the 16 objects throughout the initial hold period, suggesting that the hand shape preparation begins well in advance of the reach. This observation concurs with that of Jeannerod and Biguer (1982), who also reported early initiation of the hand shaping, preceding the onset of reach by 40–120 ms. The even earlier preshaping of the hand found in the present study may reflect the differences in the paradigms. In the previous study the subjects began each trial with their eyes closed while the object was changed. The subjects then opened their eyes and waited for a "go" cues before making a fast and accurate grasp (Jeannerod and Biguer 1982). In our task the subjects' eyes remained open throughout the experiment, and they viewed the changes in objects prior to receiving instructions as to which grasp to perform. In addition the trials were self-initiated after receiving the instructions without a time constraint. Therefore the subjects had a considerable period of time in which to adjust hand shape prior to reach.

### *Actual versus mimed grasps*

The E1s of the mimed grasps were similar to the E1s of the actual grasps, suggesting that the subjects used the same control strategy whether or not tactile contact was made. The thumb and fingers of the E1s for the mimed grasps have the same flexed posture observed for the actual power grasps and the more extended posture for the precision grasps. The temporal weightings were also similar. Therefore control strategy used for actual grasps generalizes to the control of mimed grasps, and the results suggest that tactile contact is not a dominant factor in the early shaping of the hand.

The temporal weightings for the mimed grasps are less divergent than those for the actual grasps, particularly during the object hold period. Therefore the mimed grasp hand shapes varied less throughout the reach-to-grasp than the hand shapes during actual grasp. This agrees with previous experiments in which subjects mimed the grasp adjacent to the object. The peak aperture of the mimed was smaller than during actual grasps of the objects (Goodale et al. 1994). During the actual grasp the compliance of the hand enables it to mold to the object contours (Hajian and Howe 1997). In contrast, the hand shape during mimed grasp was dependent on visual cues and memory and lacked the molding to the object. The mimed grasp lacked the same requirement of the actual grasp, that of enclosing an object. Therefore the need for accuracy in the maximum aperture and final grasp posture was most likely diminished. The net result was the more compressed temporal weightings.

### *Importance of higher synergies*

The final goal of the study was to investigate the contribution of the higher order eigenpostures to the formation of the grasp. It was previously shown that for static grasps the higher principal components contributed important information even though these components account for only a small percentage of the variance (Santello et al. 1998). The present results demonstrate that the higher order components contribute a great deal to the overall shape of the hand. The flexion of the PIPs and DIPs increased with the addition of the higher order eigenpostures. The finger flexion gradually increased across the MCPs, PIPs, or DIPs in parallel until the hand enclosed the object. Therefore not only did the higher order eigenpostures add critical details needed for static grasp but also for the act of preshaping during the grasp.

The findings in this study add to the growing evidence that the hand is controlled as a unit. There are four specific findings. First the base posture described over 97% of the variance across subjects, grasps, and objects. Second, the entire act of reach-to-grasp is specified by a temporal weighting of this base posture. Third, adding the higher order eigenpostures did not influence hand shape at the single joint or digit level but instead changed hand posture across the joints. For example, the increased flexion of the PIPs from $USV_1$ to $USV_{1–7}$ at the time of object grasp occurred in all long fingers (Fig. 7). Last, the mimed grasps can be explained by the same eigenpostures as the actual grasps indicating a common control strategy. These findings refute the traditional view that the hand is controlled at a single joint, digit, or muscle level and suggest that the CNS uses a simplifying strategy in the control of the hand during reach-to-grasp. Other control strategies may be used for other hand movements.

The simplifying control strategy detected by the SVD technique is observed at the output stage. Are these eigenpostures represented at the cortical level? The results of stimulation and lesion studies in the motor cortex are consistent with global control of the hand. Stimulation of one site in M1 evokes responses in several muscles of the hand (Donoghue et al. 1992; Sato and Tanji 1989) or movement around contiguous joints or fingers (Gould et al. 1986; Kwan et al. 1978; Strick and Preston 1978). Focal inactivations or focal strokes in the hand area of the motor cortex do not disrupt movements of individual fingers; rather, movement of different combinations are effected (Schieber 1999; Schieber and Poliakov 1998).

Single-unit recordings in primary motor and premotor cortex also suggest that the hand is controlled as a unit. In monkeys a single neuron in M1 generally discharges in relation to multiple instructed finger movements (Schieber and Hibbard 1993). Furthermore, the population of cells active with different finger movements overlaps extensively (Schieber and Hibbard 1993). Motor neurons in the ventral premotor (F5) cortex in monkeys have been shown to discharge selectively during a specific grasp such as precision grip, finger prehension, or whole hand prehension (Murata et al. 1997; Rizzolatti et al. 1988). The firing of these neurons correlated only with the specific grasps and not the individual movements made by the monkeys (Rizzolatti et al. 1988). These findings suggest that the hand is represented as a unit at the premotor cortical unit. The eigenpostures observed at the output stage may be represented in the discharge of a population of hand-related motor and premotor cortical cells.

The authors thank M. McPhee for technical and graphical assistance.

Funding was provided in part by National Institute of Neurological Disorders and Stroke Grants F32 NS-10491, R01 NS-18338, and R01 NS-31530.

## REFERENCES

ANDERSEN P, HAGAN PJ, PHILLIPS CG, AND POWELL TPS. Mapping by microstimulation of overlapping projections from area 4 to motor units of the baboon's hand. *Proc R Soc Lond B Biol Sci* 188: 31–60, 1975.

ARBIB MA, IBERALL T, AND LYONS D. Coordinated control programs for movements of the hand. *Exp Brain Res Suppl* 10: 111–129, 1985.

BOOTSMA RJ, MARTENIUK RG, MACKENZIE CL, AND ZAAL FTJM. The speed-accuracy trade-off in manual prehension: effects of movement amplitude, object size, and object width on kinematic characteristics. *Exp Brain Res* 98: 535–541, 1994.

BUYS EJ, LEMON RN, MANTEL GW, AND MUIR RB. Selective facilitation of different hand muscles by single corticospinal neurones in the conscious monkey. *J Physiol (Lond)* 381: 529–549, 1986.

CHENEY PD AND FETZ EE. Comparable patterns of muscle facilitation evoked by individual corticomotoneuronal (CM) cells and by single intracortical microstimulation in primates: evidence for functional groups of CM cells. *J Neurophysiol* 53: 786–804, 1985.

CHENEY PD, FETZ EE, AND PALMER SS. Patterns of facilitation and suppression of antagonist forelimb muscles from motor cortex sites in the awake monkey. *J Neurophysiol* 53: 805–820, 1985.

CHIEFFI S AND GENTILUCCI M. Coordination between the transport and the grasp components during prehension movements. *Exp Brain Res* 94: 471–477, 1993.

CUTKOWSKY MR AND HOWE RD. Human grasp choice and robotic grasp analysis. In: *Dextrous Robot Hands*, edited by Venkataraman ST and Iberall T. New York: Springer-Verlag, 1990, p. 5–31.

DONOGHUE JP, LEIBOVIC S, AND SANES JN. Organization of the forelimb area in squirrel monkey motor cortex: representation of digit, wrist, and elbow muscles. *Exp Brain Res* 89: 1–19, 1992.

ENGEL KC, FLANDERS M, AND SOECHTING JF. Anticipatory and sequential motor control in piano playing. *Exp Brain Res* 113: 189–199, 1997.

FLANDERS M AND SOECHTING JF. Kinematics of typing: parallel control of the two hands. *J Neurophysiol* 67: 1264–1274, 1992.

GLASER EM AND RUCHKIN DS. *Principles of Neurobiological Signal Analysis*. New York: Academic, 1967.

GOODALE MA, JAKOBSON LS, AND KEILLOR JM. Differences in the visual control of pantomimed and natural grasping movements. *Neuropsychologia* 32: 1159–1178, 1994.

GORDON AM, CASABONA A, AND SOECHTING JF. The learning of novel finger movement sequences. *J Neurophysiol* 72: 1596–1610, 1994.

GOULD HJ, CUSICK CG, PONS TP, AND KAAS JH. The relationship of corpus callosum connections to electrical stimulation maps of motor, supplementary motor and the frontal eyefields in owl monkeys. *J Comp Neurol* 247: 297–325, 1986.

HAJIAN AZ AND HOWE RD. Identification of the mechanical impedance at the human finger tip. *J Biomed Eng* 119: 109–114, 1997.

HENDLER RW AND SHRAGER RI. Deconvolutions based on singular value decomposition and the pseudoinverse: a guide for beginners. *J Biochem Biophys Methods* 28: 1–33, 1994.

IBERALL T AND FAGG A. Neural networks for selecting hand shapes. In: *Hand and Brain: The Neurophysiology and Psychology of Hand Movements*, edited by Wing AM, Haggard P, and Flanagan JR. San Diego, CA: Academic, 1996, p. 243–264.

JEANNEROD M. The timing of natural prehension movements. *J Mot Behav* 16: 235–254, 1984.

JEANNEROD M AND BIGUER B. Visuomotor mechanisms in reaching within extrapersonal space. In: *Analysis of Visual Behavior*, edited by Ingle DJ, Goodale MA, and Mansfield RJW. Cambridge, MA: MIT Press, 1982, p. 387–409.

KAMAKURA N, MATSUO M, ISHII H, MITSUBOSHI F, AND MIURA Y. Patterns of static prehension in normal hands. *Am J Occup Ther* 7: 437–445, 1980.

KAPANDJI IA. *The Physiology of the Joints. Upper Limb* (2nd ed.). London: E and S Livingstone, 1970, vol. 1, p. 146–202.

KWAN HC, MACKAY WA, MURPHY JT, AND WONG YC. Spatial organization of precentral cortex in awake primates. II. Motor outputs. *J Neurophysiol* 41: 1120–1131, 1978.

LANDSMEER JMF. The coordination of finger-joint motions. *J Bone Joint Surg* 45A: 1654–1662, 1963.

LANDSMEER JMF AND LONG C. The mechanism of finger control based on electromyograms and location analysis. *Acta Anat* 60: 330–347, 1965.

LEMON RN. Neural control of dexterity: what has been achieved? *Exp Brain Res* 128: 6–12, 1999.

LEMON RN, MANTEL GW, AND MUIR RB. Corticospinal facilitation of hand muscles during voluntary movement in the conscious monkey. *J Physiol (Lond)* 381: 529–549, 1986.

LEYTON ASF AND SHERRINGTON CS. Observations on the excitable cortex of the chimpanzee, orangutan and gorilla. *Q J Exp Physiol* 11: 137–222, 1917.

LONG C, CONRAD PW, HALL EA, AND FURLER SL. Intrinsic-extrinsic muscle control of the hand in power grip and precision handling. *J Bone Joint Surg* 52A: 853–867, 1970.

MARTENIUK RG, LEAVITT JL, MACKENZIE CL, AND ATHENES S. Functional relationships between grasp and transport components in a prehension task. *Hum Mov Sci* 9: 149–176, 1990.

MASON CR, GOMEZ JE, AND EBNER TJ. Simplifying strategies of human whole hand grasp as determined by singular value decomposition. *Soc Neurosci Abstr* 25: 113, 1999.

MCKIERNAN BJ, MARCARIO JK, KARRER JH, AND CHENEY PD. Corticomotoneuronal postspike effects in shoulder, elbow, wrist, digit, and intrinisic hand muscles during a reach and prehension task. *J Neurophysiol* 80: 1961–1980, 1998.

MURATA A, FADIGA L, FOGASSI L, GALLESE V, RAOS V, AND RIZZOLATTI R. Object representations in the ventral premotor cortex of the monkey. *J Neurophysiol* 78: 2226–2230, 1997.

NAPIER JR. The prehensile movement of the human hand. *J Bone Joint Surg* 38B: 902–913, 1956.

OLDFIELD RC. The assessment and analysis of handedness: the Edinburgh inventory. *Neuropsychologia* 9: 97–113, 1971.

PAULIGNAN Y, JEANNEROD M, MACKENZIE C, AND MARTENIUK R. Selective perturbation of visual input during prehension movements 2. The effects of changing object size. *Exp Brain Res* 87: 407–420, 1991.

PAULIGNAN Y, MACKENZIE C, MARTENIUK R, AND JEANNEROD M. The coupling of arm and finger movements during prehension. *Exp Brain Res* 79: 431–435, 1990.

PENFIELD W AND RASMUSSEN T. *The Cerebral Cortex of Man*. New York: MacMillan, 1950.

POLIAKOV AV AND SCHIEBER MH. Limited functional grouping of neurons in the motor cortex hand area during individuated finger movements: a cluster analysis. *J Neurophysiol* 82: 3488–3505, 1999.

RIZZOLATTI G, CAMARDA R, FOGASSI L, GENTILUCCI M, LUPPINO G, AND MATELLI M. Functional organization of inferior area 6 in the macaque monkey. II. Area F5 and the control of distal movement. *Exp Brain Res* 71: 491–507, 1988.

SANTELLO M, FLANDERS M, AND SOECHTING JF. Postural hand synergies for tool use. *J Neurosci* 18: 10105–10115, 1998.

SANTELLO M AND SOECHTING JF. Matching object size by controlling finger span and hand shape. *Somatosens Mot Res* 14: 203–212, 1997.

SANTELLO M AND SOECHTING JF. Gradual molding of the hand to object contours. *J Neurophysiol* 79: 1307–1320, 1998.

SATO KC AND TANJI J. Digit-muscle responses evoked from multiple intracortical foci in monkey precentral motor cortex. *J Neurophysiol* 62: 959–970, 1989.

SCHIEBER M. How might the motor cortex individuate movements? *Trends Neurosci* 13: 440–445, 1990.

SCHIEBER M. Individuated finger movements of Rhesus monkeys: a means of quantifying the independence of the digits. *J Neurophysiol* 65: 1381–1391, 1991.

SCHIEBER M. Muscular production of individuated finger movements: the roles of extrinsic finger muscles. *J Neurosci* 15: 284–297, 1995.

SCHIEBER M. Somatotopic gradients in the distributed organization of the human primary motor cortex hand area: evidence from small infarcts. *Exp Brain Res* 128: 139–148, 1999.

SCHIEBER M AND POLIAKOV AV. Partial inactivation of the primary motor cortex hand area: effects of individuated finger movements. *J Neurosci* 18: 9038–9054, 1998.

SCHIEBER MH, CHUA M, PETIT J, AND HUNT CC. Tension distribution of single motor units in multitendoned muscles: comparison of a homologous digit muscle in cats and monkeys. *J Neurosci* 17: 1734–1747, 1997.

SCHIEBER MH AND HIBBARD LS. How somatotopic is the motor cortex hand area? *Science* 261: 489–492, 1993.

SERLIN DM AND SCHIEBER M. Morphological regions of the multitendoned extrinsic finger muscles in the monkey forearm. *Acta Anat* 14: 255–266, 1993.

SOECHTING JF AND FLANDERS M. Flexibility and repeatability of finger movements during typing: analysis of multiple degrees of freedom. *J Comput Neurosci* 4: 29–46, 1997.

STRICK PL AND PRESTON JB. Multiple representation in the primate motor cortex. *Brain Res* 154: 366–370, 1978.

TUBIANA R. Architecture and function of the hand. In: *The Hand*, edited by Tubiana R. Philadelphia, PA: Saunders, 1981, vol. 1, p. 19–93.

WOOLSEY CN. Organization of somatic sensory and motor areas of the cerebral cortex. In: *Biological and Biochemical Bases of Behavior*, edited by Harlow HF and Woolsey CN. Madison, WI: Univ. of Wisconsin Press, 1958, p. 63–81.

WOOLSEY CN, ERICKSON TC, AND GILSON WE. Localization in somatic sensory and motor areas of human cerebral cortex as determined by direct recordings of evoked potentials and electrical stimulation. *J Neurosurg* 51: 476–506, 1979.